Observation of the decays $\chi_{cJ} \to \phi\phi\eta$

M. Ablikim,[1] M. N. Achasov,[10,a] P. Adlarson,[63] S. Ahmed,[15] M. Albrecht,[4] M. Alekseev,[62a,62c] A. Amoroso,[62a,62c] F. F. An,[1] Q. An,[59,47] Y. Bai,[46] O. Bakina,[28] R. Baldini Ferroli,[23a] I. Balossino,[24a] Y. Ban,[37,b] K. Begzsuren,[26] J. V. Bennett,[5] N. Berger,[27] M. Bertani,[23a] D. Bettoni,[24a] F. Bianchi,[62a,62c] J. Biernat,[63] J. Bloms,[56] I. Boyko,[28] R. A. Briere,[5] H. Cai,[64] X. Cai,[1,47] A. Calcaterra,[23a] G. F. Cao,[1,51] N. Cao,[1,51] S. A. Cetin,[50b] J. Chai,[62c] J. F. Chang,[1,47] W. L. Chang,[1,51] G. Chelkov,[28,c,d] D. Y. Chen,[6] G. Chen,[1] H. S. Chen,[1,51] J. Chen,[16] M. L. Chen,[1,47] S. J. Chen,[35] X. R. Chen,[25] Y. B. Chen,[1,47] W. Cheng,[62c] G. Cibinetto,[24a] F. Cossio,[62c] X. F. Cui,[36] H. L. Dai,[1,47] J. P. Dai,[41,e] X. C. Dai,[1,51] A. Dbeyssi,[15] D. Dedovich,[28] Z. Y. Deng,[1] A. Denig,[27] I. Denysenko,[28] M. Destefanis,[62a,62c] F. De Mori,[62a,62c] Y. Ding,[33] C. Dong,[36] J. Dong,[1,47] L. Y. Dong,[1,51] M. Y. Dong,[1,47,51] Z. L. Dou,[35] S. X. Du,[67] J. Z. Fan,[49,†] J. Fang,[1,47] S. S. Fang,[1,51] Y. Fang,[1] R. Farinelli,[24a,24b] L. Fava,[62b,62c] F. Feldbauer,[4] G. Felici,[23a] C. Q. Feng,[59,47] M. Fritsch,[4] C. D. Fu,[1] Y. Fu,[1] Q. Gao,[1] X. L. Gao,[59,47] Y. Gao,[60] Y. Gao,[49] Y. G. Gao,[6] B. Garillon,[27] I. Garzia,[24a] E. M. Gersabeck,[54] A. Gilman,[55] K. Goetzen,[11] L. Gong,[36] W. X. Gong,[1,47] W. Gradl,[27] M. Greco,[62a,62c] L. M. Gu,[35] M. H. Gu,[1,47] S. Gu,[2] Y. T. Gu,[13] A. Q. Guo,[22] L. B. Guo,[34] R. P. Guo,[39] Y. P. Guo,[27] A. Guskov,[28] S. Han,[64] X. Q. Hao,[16] F. A. Harris,[52] K. L. He,[1,51] F. H. Heinsius,[4] T. Held,[4] Y. K. Heng,[1,47,51] M. Himmelreich,[11,f] Y. R. Hou,[51] Z. L. Hou,[1] H. M. Hu,[1,51] J. F. Hu,[41,e] T. Hu,[1,47,51] Y. Hu,[1] G. S. Huang,[59,47] J. S. Huang,[16] X. T. Huang,[40] X. Z. Huang,[35] N. Huesken,[56] T. Hussain,[61] W. Ikegami Andersson,[63] W. Imoehl,[22] M. Irshad,[59,47] Q. Ji,[1] Q. P. Ji,[16] X. B. Ji,[1,51] X. L. Ji,[1,47] H. L. Jiang,[40] X. S. Jiang,[1,47,51] X. Y. Jiang,[36] J. B. Jiao,[40] Z. Jiao,[18] D. P. Jin,[1,47,51] S. Jin,[35] Y. Jin,[53] T. Johansson,[63] N. Kalantar-Nayestanaki,[30] X. S. Kang,[33] R. Kappert,[30] M. Kavatsyuk,[30] B. C. Ke,[42,1] I. K. Keshk,[4] A. Khoukaz,[56] P. Kiese,[27] R. Kiuchi,[1] R. Kliemt,[11] L. Koch,[29] O. B. Kolcu,[50b,g] B. Kopf,[4] M. Kuemmel,[4] M. Kuessner,[4] A. Kupsc,[63] M. Kurth,[1] M. G. Kurth,[1,51] W. Kühn,[29] J. S. Lange,[29] P. Larin,[15] L. Lavezzi,[62c] H. Leithoff,[27] T. Lenz,[27] C. Li,[38] C. H. Li,[32] Cheng Li,[59,47] D. M. Li,[67] F. Li,[1,47] G. Li,[1] H. B. Li,[1,51] H. J. Li,[9,*,h] J. C. Li,[1] Ke Li,[1] L. K. Li,[1] Lei Li,[3] P. L. Li,[59,47] P. R. Li,[31] W. D. Li,[1,51] W. G. Li,[1] X. H. Li,[59,47] X. L. Li,[40] X. N. Li,[1,47] Z. B. Li,[48] Z. Y. Li,[48] H. Liang,[1,51] H. Liang,[59,47] Y. F. Liang,[44] Y. T. Liang,[25] G. R. Liao,[12] L. Z. Liao,[1,51] J. Libby,[21] C. X. Lin,[48] D. X. Lin,[15] Y. J. Lin,[13] B. Liu,[41,e] B. J. Liu,[1] C. X. Liu,[1] D. Liu,[59,47] D. Y. Liu,[41,e] F. H. Liu,[43] Fang Liu,[1] Feng Liu,[6] H. B. Liu,[13] H. M. Liu,[1,51] Huanhuan Liu,[1] Huihui Liu,[17] J. B. Liu,[59,47] J. Y. Liu,[1,51] K. Liu,[1] K. Y. Liu,[33] Ke Liu,[6] L. Y. Liu,[13] Q. Liu,[51] S. B. Liu,[59,47] T. Liu,[1,51] X. Liu,[31] X. Y. Liu,[1,51] Y. B. Liu,[36] Z. A. Liu,[1,47,51] Zhiqing Liu,[40] Y. F. Long,[37,b] X. C. Lou,[1,47,51] H. J. Lu,[18] J. D. Lu,[1,51] J. G. Lu,[1,47] Y. Lu,[1] Y. P. Lu,[1,47] C. L. Luo,[34] M. X. Luo,[66] P. W. Luo,[48] T. Luo,[9‡,h] X. L. Luo,[1,47] S. Lusso,[62c] X. R. Lyu,[51] F. C. Ma,[33] H. L. Ma,[1] L. L. Ma,[40] M. M. Ma,[1,51] Q. M. Ma,[1] X. N. Ma,[36] X. X. Ma,[1,51] X. Y. Ma,[1,47] Y. M. Ma,[40] F. E. Maas,[15] M. Maggiora,[62a,62c] S. Maldaner,[27] S. Malde,[57] Q. A. Malik,[61] A. Mangoni,[23b] Y. J. Mao,[37,b] Z. P. Mao,[1] S. Marcello,[62a,62c] Z. X. Meng,[53] J. G. Messchendorp,[30] G. Mezzadri,[24a] J. Min,[1,47] T. J. Min,[35] R. E. Mitchell,[22] X. H. Mo,[1,47,51] Y. J. Mo,[6] C. Morales Morales,[15] N. Yu. Muchnoi,[10,a] H. Muramatsu,[55] A. Mustafa,[4] S. Nakhoul,[11,f] Y. Nefedov,[28] F. Nerling,[11,f] I. B. Nikolaev,[10,a] Z. Ning,[1,47] S. Nisar,[8,i] S. L. Niu,[1,47] S. L. Olsen,[51] Q. Ouyang,[1,47,51] S. Pacetti,[23b] Y. Pan,[59,47] M. Papenbrock,[63] P. Patteri,[23a] M. Pelizaeus,[4] H. P. Peng,[59,47] K. Peters,[11,f] J. Pettersson,[63] J. L. Ping,[34] R. G. Ping,[1,51] A. Pitka,[4] R. Poling,[55] V. Prasad,[59,47] M. Qi,[35] S. Qian,[1,47] C. F. Qiao,[51] X. P. Qin,[13] X. S. Qin,[4] Z. H. Qin,[1,47] J. F. Qiu,[1] S. Q. Qu,[36] K. H. Rashid,[61,j] K. Ravindran,[21] C. F. Redmer,[27] M. Richter,[4] A. Rivetti,[62c] V. Rodin,[30] M. Rolo,[62c] G. Rong,[1,51] Ch. Rosner,[15] M. Rump,[56] A. Sarantsev,[28,k] M. Savrié,[24b] Y. Schelhaas,[27] K. Schoenning,[63] W. Shan,[19] X. Y. Shan,[59,47] M. Shao,[59,47] C. P. Shen,[2] P. X. Shen,[36] X. Y. Shen,[1,51] H. Y. Sheng,[1] X. Shi,[1,47] X. D. Shi,[59,47] J. J. Song,[40] Q. Q. Song,[59,47] X. Y. Song,[1] S. Sosio,[62a,62c] C. Sowa,[4] S. Spataro,[62a,62c] F. F. Sui,[40] G. X. Sun,[1] J. F. Sun,[16] L. Sun,[64] S. S. Sun,[1,51] X. H. Sun,[1] Y. J. Sun,[59,47] Y. K. Sun,[59,47] Y. Z. Sun,[1] Z. J. Sun,[1,47] Z. T. Sun,[1] Y. T. Tan,[59,47] C. J. Tang,[44] G. Y. Tang,[1] X. Tang,[1] V. Thoren,[63] B. Tsednee,[26] I. Uman,[50d] B. Wang,[1] B. L. Wang,[51] C. W. Wang,[35] D. Y. Wang,[37,b] K. Wang,[1,47] L. L. Wang,[1] L. S. Wang,[1] M. Wang,[40] M. Z. Wang,[37,b] Meng Wang,[1,51] P. L. Wang,[1] R. M. Wang,[65] W. P. Wang,[59,47] X. Wang,[37,b] X. F. Wang,[1] X. L. Wang,[9,h] Y. Wang,[48] Y. Wang,[59,47] Y. F. Wang,[1,47,51] Y. Q. Wang,[1] Z. Wang,[1,47] Z. G. Wang,[1,47] Z. Y. Wang,[51] Z. Y. Wang,[1] Zongyuan Wang,[1,51] T. Weber,[4] D. H. Wei,[12] P. Weidenkaff,[27] F. Weidner,[56] H. W. Wen,[34] S. P. Wen,[1] U. Wiedner,[4] G. Wilkinson,[57] M. Wolke,[63] L. H. Wu,[1] L. J. Wu,[1,51] Z. Wu,[1,47] L. Xia,[59,47] Y. Xia,[20] S. Y. Xiao,[1] Y. J. Xiao,[1,51] Z. J. Xiao,[34] Y. G. Xie,[1,47] Y. H. Xie,[6] T. Y. Xing,[1,51] X. A. Xiong,[1,51] Q. L. Xiu,[1,47] G. F. Xu,[1] J. J. Xu,[35] L. Xu,[1] Q. J. Xu,[14] W. Xu,[1,51] X. P. Xu,[45] F. Yan,[60] L. Yan,[62a,62c] W. B. Yan,[59,47] W. C. Yan,[2] Y. H. Yan,[20] H. J. Yang,[41,e] H. X. Yang,[1] L. Yang,[64] R. X. Yang,[59,47] S. L. Yang,[1,51] Y. H. Yang,[35] Y. X. Yang,[12] Yifan Yang,[1,51] Z. Q. Yang,[20] Zhi Yang,[25] M. Ye,[1,47] M. H. Ye,[7] J. H. Yin,[1] Z. Y. You,[48] B. X. Yu,[1,47,51] C. X. Yu,[36] J. S. Yu,[20] T. Yu,[60] C. Z. Yuan,[1,51] X. Q. Yuan,[37,b] Y. Yuan,[1] C. X. Yue,[32] A. Yuncu,[50b,l] A. A. Zafar,[61] Y. Zeng,[20] B. X. Zhang,[1] B. Y. Zhang,[1,47] C. C. Zhang,[1] D. H. Zhang,[1] H. H. Zhang,[48] H. Y. Zhang,[1,47] J. Zhang,[1,51] J. L. Zhang,[65] J. Q. Zhang,[4] J. W. Zhang,[1,47,51] J. Y. Zhang,[1] J. Z. Zhang,[1,51] K. Zhang,[1,51] L. Zhang,[1] Lei Zhang,[35] S. F. Zhang,[35] T. J. Zhang,[41,e] X. Y. Zhang,[40] Y. Zhang,[59,47] Y. H. Zhang,[1,47] Y. T. Zhang,[59,47] Yang Zhang,[1] Yao Zhang,[1] Yi Zhang,[9,h] Yu Zhang,[51] Z. H. Zhang,[6] Z. P. Zhang,[59] Z. Y. Zhang,[64] G. Zhao,[1] J. Zhao,[32] J. W. Zhao,[1,47] J. Y. Zhao,[1,51] J. Z. Zhao,[1,47]

Lei Zhao,[59,47] Ling Zhao,[1] M. G. Zhao,[36] Q. Zhao,[1] S. J. Zhao,[67] T. C. Zhao,[1] Y. B. Zhao,[1,47] Z. G. Zhao,[59,47] A. Zhemchugov,[28,c] B. Zheng,[60] J. P. Zheng,[1,47] Y. Zheng,[37,b] Y. H. Zheng,[51] B. Zhong,[34] L. Zhou,[1,47] L. P. Zhou,[1,51] Q. Zhou,[1,51] X. Zhou,[64] X. K. Zhou,[51] X. R. Zhou,[59,47] Xiaoyu Zhou,[20] Xu Zhou,[20] A. N. Zhu,[1,51] J. Zhu,[36] J. Zhu,[48] K. Zhu,[1] K. J. Zhu,[1,47,51] S. H. Zhu,[58] W. J. Zhu,[36] X. L. Zhu,[49] Y. C. Zhu,[59,47] Y. S. Zhu,[1,51] Z. A. Zhu,[1,51] J. Zhuang,[1,47] B. S. Zou,[1] and J. H. Zou[1]

(BESIII Collaboration)

[1]*Institute of High Energy Physics, Beijing 100049, People's Republic of China*
[2]*Beihang University, Beijing 100191, People's Republic of China*
[3]*Beijing Institute of Petrochemical Technology, Beijing 102617, People's Republic of China*
[4]*Bochum Ruhr-University, D-44780 Bochum, Germany*
[5]*Carnegie Mellon University, Pittsburgh, Pennsylvania 15213, USA*
[6]*Central China Normal University, Wuhan 430079, People's Republic of China*
[7]*China Center of Advanced Science and Technology, Beijing 100190, People's Republic of China*
[8]*COMSATS University Islamabad, Lahore Campus, Defence Road, Off Raiwind Road, 54000 Lahore, Pakistan*
[9]*Fudan University, Shanghai 200443, People's Republic of China*
[10]*G.I. Budker Institute of Nuclear Physics SB RAS (BINP), Novosibirsk 630090, Russia*
[11]*GSI Helmholtzcentre for Heavy Ion Research GmbH, D-64291 Darmstadt, Germany*
[12]*Guangxi Normal University, Guilin 541004, People's Republic of China*
[13]*Guangxi University, Nanning 530004, People's Republic of China*
[14]*Hangzhou Normal University, Hangzhou 310036, People's Republic of China*
[15]*Helmholtz Institute Mainz, Johann-Joachim-Becher-Weg 45, D-55099 Mainz, Germany*
[16]*Henan Normal University, Xinxiang 453007, People's Republic of China*
[17]*Henan University of Science and Technology, Luoyang 471003, People's Republic of China*
[18]*Huangshan College, Huangshan 245000, People's Republic of China*
[19]*Hunan Normal University, Changsha 410081, People's Republic of China*
[20]*Hunan University, Changsha 410082, People's Republic of China*
[21]*Indian Institute of Technology Madras, Chennai 600036, India*
[22]*Indiana University, Bloomington, Indiana 47405, USA*
[23a]*INFN Laboratori Nazionali di Frascati, I-00044, Frascati, Italy*
[23b]*INFN and University of Perugia, I-06100, Perugia, Italy*
[24a]*INFN Sezione di Ferrara, I-44122, Ferrara, Italy*
[24b]*University of Ferrara, I-44122, Ferrara, Italy*
[25]*Institute of Modern Physics, Lanzhou 730000, People's Republic of China*
[26]*Institute of Physics and Technology, Peace Avenue 54B, Ulaanbaatar 13330, Mongolia*
[27]*Johannes Gutenberg University of Mainz, Johann-Joachim-Becher-Weg 45, D-55099 Mainz, Germany*
[28]*Joint Institute for Nuclear Research, 141980 Dubna, Moscow Region, Russia*
[29]*Justus-Liebig-Universitaet Giessen, II. Physikalisches Institut, Heinrich-Buff-Ring 16, D-35392 Giessen, Germany*
[30]*KVI-CART, University of Groningen, NL-9747 AA Groningen, The Netherlands*
[31]*Lanzhou University, Lanzhou 730000, People's Republic of China*
[32]*Liaoning Normal University, Dalian 116029, People's Republic of China*
[33]*Liaoning University, Shenyang 110036, People's Republic of China*
[34]*Nanjing Normal University, Nanjing 210023, People's Republic of China*
[35]*Nanjing University, Nanjing 210093, People's Republic of China*
[36]*Nankai University, Tianjin 300071, People's Republic of China*
[37]*Peking University, Beijing 100871, People's Republic of China*
[38]*Qufu Normal University, Qufu 273165, People's Republic of China*
[39]*Shandong Normal University, Jinan 250014, People's Republic of China*
[40]*Shandong University, Jinan 250100, People's Republic of China*
[41]*Shanghai Jiao Tong University, Shanghai 200240, People's Republic of China*
[42]*Shanxi Normal University, Linfen 041004, People's Republic of China*
[43]*Shanxi University, Taiyuan 030006, People's Republic of China*
[44]*Sichuan University, Chengdu 610064, People's Republic of China*
[45]*Soochow University, Suzhou 215006, People's Republic of China*
[46]*Southeast University, Nanjing 211100, People's Republic of China*
[47]*State Key Laboratory of Particle Detection and Electronics, Beijing 100049, Hefei 230026, People's Republic of China*

[48]*Sun Yat-Sen University, Guangzhou 510275, People's Republic of China*
[49]*Tsinghua University, Beijing 100084, People's Republic of China*
[50a]*Ankara University, 06100 Tandogan, Ankara, Turkey*
[50b]*Istanbul Bilgi University, 34060 Eyup, Istanbul, Turkey*
[50c]*Uludag University, 16059 Bursa, Turkey*
[50d]*Near East University, Nicosia, North Cyprus, Mersin 10, Turkey*
[51]*University of Chinese Academy of Sciences, Beijing 100049, People's Republic of China*
[52]*University of Hawaii, Honolulu, Hawaii 96822, USA*
[53]*University of Jinan, Jinan 250022, People's Republic of China*
[54]*University of Manchester, Oxford Road, Manchester, M13 9PL, United Kingdom*
[55]*University of Minnesota, Minneapolis, Minnesota 55455, USA*
[56]*University of Muenster, Wilhelm-Klemm-Street 9, 48149 Muenster, Germany*
[57]*University of Oxford, Keble Road, Oxford, United Kingdom OX13RH*
[58]*University of Science and Technology Liaoning, Anshan 114051, People's Republic of China*
[59]*University of Science and Technology of China, Hefei 230026, People's Republic of China*
[60]*University of South China, Hengyang 421001, People's Republic of China*
[61]*University of the Punjab, Lahore-54590, Pakistan*
[62a]*University of Turin, I-10125, Turin, Italy*
[62b]*University of Eastern Piedmont, I-15121, Alessandria, Italy*
[62c]*INFN, I-10125, Turin, Italy*
[63]*Uppsala University, Box 516, SE-75120 Uppsala, Sweden*
[64]*Wuhan University, Wuhan 430072, People's Republic of China*
[65]*Xinyang Normal University, Xinyang 464000, People's Republic of China*
[66]*Zhejiang University, Hangzhou 310027, People's Republic of China*
[67]*Zhengzhou University, Zhengzhou 450001, People's Republic of China*

(Received 10 November 2019; published 24 January 2020)

Using a data sample of $(448.1 \pm 2.9) \times 10^6$ $\psi(3686)$ decays collected by the BESIII detector at the Beijing Electron Positron Collider (BEPCII), we observe the decays $\chi_{cJ} \to \phi\phi\eta\,(J = 0, 1, 2)$, where the χ_{cJ} are produced via the radiative processes $\psi(3686) \to \gamma\chi_{cJ}$. The branching fractions are measured to be $\mathcal{B}(\chi_{c0} \to \phi\phi\eta) = (8.41 \pm 0.74 \pm 0.62) \times 10^{-4}$, $\mathcal{B}(\chi_{c1} \to \phi\phi\eta) = (2.96 \pm 0.43 \pm 0.22) \times 10^{-4}$, and $\mathcal{B}(\chi_{c2} \to \phi\phi\eta) = (5.33 \pm 0.52 \pm 0.39) \times 10^{-4}$, where the first uncertainties are statistical, and the second are systematic. We also search for intermediate states in the $\phi\phi$ or $\eta\phi$ subsystems, but no significant structure is seen due to the limited statistics.

DOI: 10.1103/PhysRevD.101.012012

[*]Corresponding author.
lihuijing@fudan.edu.cn
[†]Corresponding author.
fjz@mail.tsinghua.edu.cn
[‡]Corresponding author.
luot@fudan.edu.cn
[a]Also at the Novosibirsk State University, Novosibirsk, 630090, Russia.
[b]Also at State Key Laboratory of Nuclear Physics and Technology, Peking University, Beijing 100871, People's Republic of China.
[c]Also at the Moscow Institute of Physics and Technology, Moscow 141700, Russia.
[d]Also at the Functional Electronics Laboratory, Tomsk State University, Tomsk, 634050, Russia.
[e]Also at Key Laboratory for Particle Physics, Astrophysics and Cosmology, Ministry of Education; Shanghai Key Laboratory for Particle Physics and Cosmology; Institute of Nuclear and Particle Physics, Shanghai 200240, People's Republic of China.
[f]Also at Goethe University Frankfurt, 60323 Frankfurt am Main, Germany.
[g]Also at Istanbul Arel University, 34295 Istanbul, Turkey.
[h]Also at Key Laboratory of Nuclear Physics and Ion-Beam Application (MOE) and Institute of Modern Physics, Fudan University, Shanghai 200443, People's Republic of China.
[i]Also at Harvard University, Department of Physics, Cambridge, Massachusetts 02138, USA.
[j]Also at Government College Women University, Sialkot—51310, Punjab, Pakistan.
[k]Also at the NRC "Kurchatov Institute," PNPI, 188300, Gatchina, Russia.
[l]Also at Bogazici University, 34342 Istanbul, Turkey.

I. INTRODUCTION

Studies of the properties of $c\bar{c}$ states play an important role in understanding the interplay between perturbative and nonperturbative effects in quantum chromodynamics (QCD). Besides J/ψ and $\psi(3686)$ decays [1], the decays of the χ_{cJ} ($J = 0, 1, 2$) [2,3] are also valuable to probe a wide variety of QCD phenomena.

To date, only a few measurements have been performed for decays of the form $\chi_{cJ} \to VVP$, where V and P denote vector and pseudoscalar mesons, respectively [1], and no measurement of the branching fraction for $\chi_{cJ} \to \phi\phi\eta$ has previously been reported. The interest in these final states arises from the search for glueballs in the $\phi\phi$ invariant mass ($M_{\phi\phi}$) spectrum. A previous partial wave analysis of the decay $J/\psi \to \gamma\phi\phi$ decay by the BESIII Collaboration [4] confirmed the existence of the $\eta(2225)$ and observed the three tensor states $f_2(2010)$, $f_2(2300)$ and $f_2(2340)$, which were first observed in the process $\pi^- p \to \phi\phi n$ [5]. Different experiments also searched for glueballs decaying to $\phi\phi$ in B decays [6], but none have so far been observed [7]. Although there are no theoretical expectations, the decays $\chi_{cJ} \to \phi\phi\eta$ may contain contributions from intermediate states decaying to $\phi\phi$ and $\eta\phi$, and observations of the same resonances as those in J/ψ decays would provide supplementary and conclusive information regarding their existence.

Due to abundant χ_{cJ} production in $\psi(3686)$ radiative decays [1], the BESIII experiment provides an ideal place to search for new χ_{cJ} decays. The BESIII detector has collected $(448.1 \pm 2.9) \times 10^6$ $\psi(3686)$ decays [8], which is the world's largest data sample of $\psi(3686)$ decays produced in e^+e^- annihilation. In this paper, we report the first measurements of the branching fractions of χ_{cJ} decays to $\phi\phi\eta$. The ϕ meson can be reconstructed with $\phi \to K^+K^-$, $\phi \to \pi^+\pi^-\pi^0$ and $\phi \to K^0_S K^0_L$ decays, and the η meson with $\eta \to \gamma\gamma$ and $\eta \to \pi^+\pi^-\pi^0$ decays. Compared to the $\phi \to K^+K^-$ and $\eta \to \gamma\gamma$ modes, other decay modes suffer from higher backgrounds and lower detection efficiencies. So in this analysis, the two ϕ mesons and the η meson are reconstructed with $\phi \to K^+K^-$ and $\eta \to \gamma\gamma$ processes.

II. DETECTOR AND MONTE CARLO SIMULATIONS

The BESIII detector is a magnetic spectrometer [9] located at the Beijing Electron Positron Collider (BEPCII) [10]. The cylindrical core of the BESIII detector consists of a helium-based multilayer drift chamber (MDC), a plastic scintillator time-of-flight system (TOF), and a CsI(Tl) electromagnetic calorimeter (EMC), which are all enclosed in a superconducting solenoidal magnet providing a 1.0 T magnetic field. The solenoid is supported by an octagonal flux-return yoke with resistive plate counter muon identifier modules interleaved with steel. The acceptance for charged particles and photons is 93% over a 4π solid angle. The momentum resolution for charged particles at 1 GeV/c is 0.5%, and the dE/dx resolution is 6% for the electrons from Bhabha scattering. The EMC measures photon energies with a resolution of 2.5% (5%) at 1 GeV in the barrel (end cap) region. The time resolution of the TOF barrel part is 68 ps, while that of the end cap part is 110 ps.

Large samples of simulated events are produced with a GEANT4-based [11] Monte Carlo (MC) package that includes the geometric description of the BESIII detector and the detector response. These samples are used to determine the detection efficiency and to estimate the backgrounds. The simulation includes the beam energy spread and initial state radiation (ISR) in the e^+e^- annihilation modeled with the generator KKMC [12]. The "inclusive" MC sample consists of the production of the $\psi(3686)$ resonance, the ISR production of the J/ψ, and the continuum processes incorporated in KKMC [12]. The known decay modes are modeled with EvtGen [13] using branching fractions taken from the Particle Data Group [1], and the remaining unknown decays of the charmonium states are modeled with LUNDCHARM [14]. The final state radiation (FSR) from charged final state particles is simulated with the PHOTOS package [15].

For the signal MC samples, the $\psi(3686) \to \gamma\chi_{cJ}$ decays are generated with the electric dipole (E1) transition [16,17] assumption, where the angular distribution is $1 + \lambda\cos^2\vartheta$ [18,19]. Here, ϑ is the polar angle of the radiative photon in the rest frame of the $\psi(3686)$ meson, and λ is $1, -1/3, 1/13$ for $J = 0, 1, 2$, respectively. The processes $\chi_{cJ} \to \phi\phi\eta$ and $\eta \to \gamma\gamma$ are generated uniformly in phase space.

III. EVENT SELECTION

The cascade decay of interest is $\psi(3686) \to \gamma\chi_{cJ}, \chi_{cJ} \to \phi\phi\eta$, with $\phi \to K^+K^-$ and $\eta \to \gamma\gamma$. Candidate events are required to have four charged tracks with zero net charge and at least three photons. Charged tracks in an event are required to have a polar angle θ with respect to the beam direction within the MDC acceptance $|\cos\theta| < 0.93$, and a distance of closest approach to the interaction point within 10 cm along the beam direction and 1 cm in the plane transverse to the beam direction. The TOF and dE/dx information are combined to evaluate particle identification (PID) confidence levels for the π and K hypotheses, and the particle type with the higher confidence level is assigned to each track. All charged tracks must be identified as kaons. Electromagnetic showers are reconstructed from clusters of energy deposited in the EMC. The energy deposited in nearby TOF counters is included to improve the reconstruction efficiency and energy resolution. Photon candidates must have a minimum energy of 25 MeV in the barrel region ($|\cos\theta| < 0.80$) or 50 MeV in the end cap region ($0.86 < |\cos\theta| < 0.92$). To exclude showers from

charged particles, a photon must be separated by at least 10° from the nearest charged track. The measured EMC time is required to be within 0 and 700 ns of the collision time to suppress electronic noise and energy deposits unrelated to the event of interest.

A four-constraint (4C) kinematic fit imposing overall energy-momentum conservation is performed with the $\gamma\gamma\gamma K^+K^-K^+K^-$ hypothesis, and the events with $\chi^2_{\rm 4C} < 40$ are retained. The requirement is based on the optimization of the figure of merit (FOM), FOM $\equiv N_{\rm sig}/\sqrt{N_{\rm tot}}$, where $N_{\rm sig}$ and $N_{\rm tot}$ are the number of signal events and total number of events estimated from the signal MC sample and data, respectively. For events with more than three photon candidates, the combination with the smallest $\chi^2_{\rm 4C}$ is retained. Further selection criteria are based on the four-momentum updated by the kinematic fit.

After the above requirements, the η candidate is reconstructed in its decay to $\gamma\gamma$ using the $\gamma\gamma$ pair with invariant mass $M_{\gamma\gamma}$ closest to the nominal η mass [1]. The η signal region is defined as $0.52 \le M_{\gamma\gamma} \le 0.58$ GeV/c^2, with its half width approximately three times larger than the detector resolution ($\sigma_\eta = 10$ MeV/c^2). Figure 1(a) shows a fit to the $M_{\gamma\gamma}$ distribution. In the fit, the signal shape is modeled by the MC-simulated line shape convolved with a Gaussian function with free width and the background is described by a linear function. The two signal ϕ candidates are chosen from the combination with the minimum value of $\Delta M^2 = (M_{K^+_iK^-_j} - m_\phi)^2 + (M_{K^+_{1-i}K^-_{1-j}} - m_\phi)^2$, where $M_{K^+K^-}$ is the invariant mass of K^+K^-, m_ϕ is the nominal ϕ mass [1], and i, j can be 0 or 1. In each event, one of the ϕ candidates is randomly chosen to be ϕ_1 with the other ϕ_2. MC studies show that the miscombination rates for both η and ϕ candidates are no more than 0.1%. The ϕ signal region is defined as $1.005 \le M_{K^+K^-} \le 1.035$ GeV/c^2, with its half width about three times the sum of the detector resolution ($\sigma_\phi = 1$ MeV/c^2) and intrinsic width [1]. Figure 1(b) shows the fit to the $M_{K^+K^-}$ distribution obtained when one of the two combinations is randomly selected. In the fit, the signal shape is modeled as a P-wave Breit-Wigner convolved with a Gaussian function, and the background shape is represented by the function $b(M_{K^+K^-}) = (M_{K^+K^-} - 2m_K)^c e^{-dM_{K^+K^-}}$, where m_K is the nominal K mass [1], and c and d are free parameters. The two-dimensional (2D) ϕ signal region is shown as the area A in Fig. 2, where $M_{K^+K^-(1)}$ and $M_{K^+K^-(2)}$ denote the invariant masses of the randomly assigned $K^+K^-(1)$ and $K^+K^-(2)$, respectively.

The mass recoiling against the η is required to be less than 3.05 GeV/c^2 to suppress background from the decay $\psi(3686) \to \eta J/\psi, J/\psi \to \gamma\phi\phi$. All combinations of $M_{\gamma\gamma}$ are required to be outside the range $[0.115, 0.150]$ GeV/c^2 to suppress background events with π^0 decays, and the invariant mass of $\gamma\eta$ must be outside the range

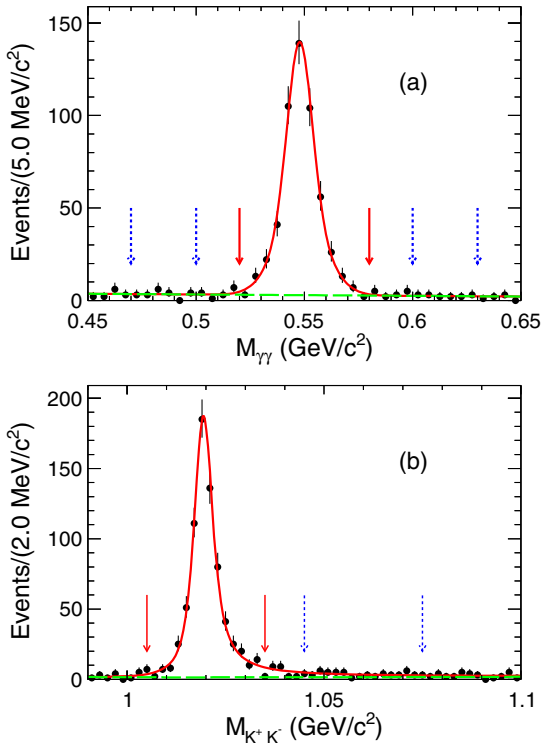

FIG. 1. Fits to (a) $M_{\gamma\gamma}$ and (b) $M_{K^+K^-}$, where one of the two combinations is randomly selected. The dots with error bars are from data, the red lines are the best fit results, and the long dashed green lines are the background shapes. The red arrows show the signal region, and the dashed blue arrows show the sideband regions.

$[1.00, 1.04]$ GeV/c^2 to suppress background from the decay $\psi(3686) \to \phi\phi\phi$, where one ϕ decays to $\gamma\eta$.

A total of 495 candidate events survive in the R1 region, which corresponds to the area A with $M_{\gamma\gamma}$ in the signal region, as shown in Fig. 3(a). The distributions

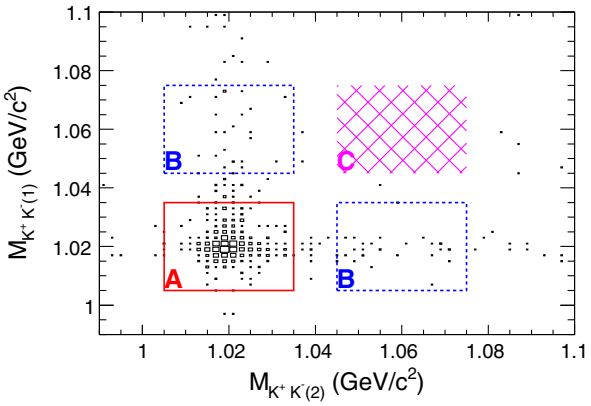

FIG. 2. Distribution of $M_{K^+K^-(1)}$ vs $M_{K^+K^-(2)}$. The solid red rectangle (area A) and dashed blue rectangles (areas B) denote the 2D ϕ signal region and 2D ϕ sideband regions, respectively. The hatched pink rectangle (area C) is where both $M_{K^+K^-(1)}$ and $M_{K^+K^-(2)}$ lie in the ϕ sideband region.

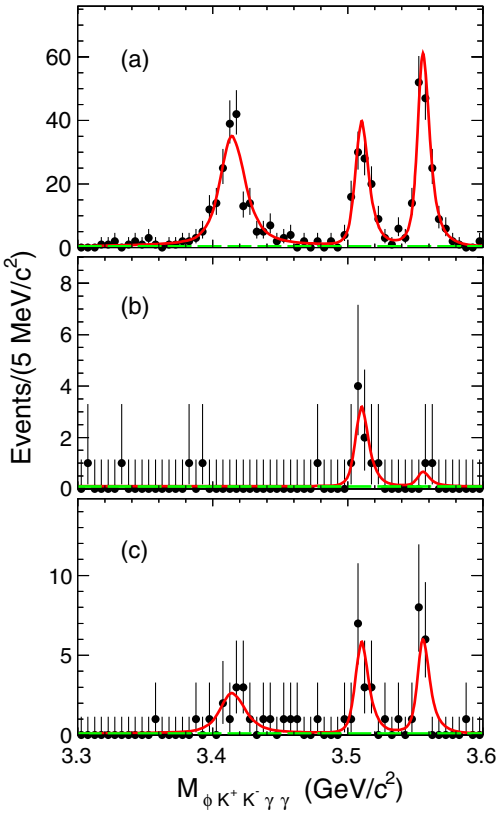

FIG. 3. Fits to the $M_{\phi K^+K^-\gamma\gamma}$ distributions for (a) the R1 region, (b) the R2 region, and (c) the R3 region. The dots with error bars are from data, the solid red lines are the best fit results, and the long dashed green lines are the fitted backgrounds.

of $M^2_{\eta\phi_1}$ vs $M^2_{\eta\phi_2}$ from the three χ_{cJ} states are depicted in Fig. 4, where the signal regions of χ_{c0}, χ_{c1}, and χ_{c2} are defined as [3.38, 3.45], [3.48, 3.54], and [3.54, 3.60] GeV/c^2 for the invariant mass $M_{\phi\phi\eta}$, respectively.

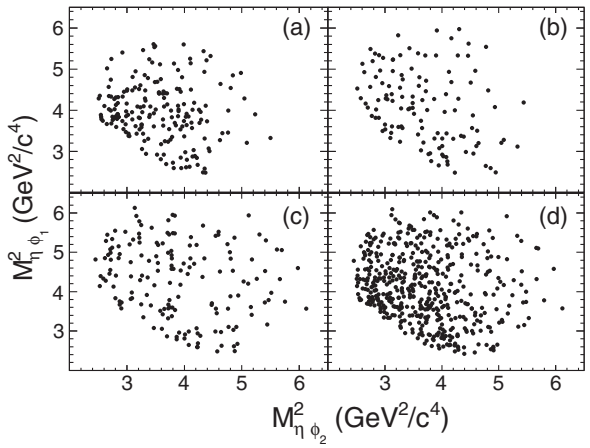

FIG. 4. Distributions of $M^2_{\eta\phi_1}$ vs $M^2_{\eta\phi_2}$ for $\chi_{cJ} \to \phi\phi\eta$ decays within the signal regions of (a) χ_{c0}, (b) χ_{c1}, and (c) χ_{c2}, as well as (d) the overall region [3.3, 3.6] GeV/c^2.

IV. BACKGROUND AND SIGNAL YIELDS

According to a study of the inclusive MC sample, consisting of 5.06×10^8 $\psi(3686)$ decays, the background sources can be categorized into two classes. Class I background is from events that do not form an η signal in the $M_{\gamma\gamma}$ distribution. This background is estimated using events in the η sideband regions of $M_{\gamma\gamma} \in [0.47, 0.50] \cup [0.60, 0.63]$ GeV/c^2. Class II background arises from decays having only one ϕ present, which is described using events in the 2D ϕ sideband regions (the areas B of Fig. 2), where one $M_{K^+K^-}$ lies in the ϕ signal region and the other is in the ϕ sideband region of $M_{K^+K^-} \in [1.045, 1.075]$ GeV/c^2. Since there are no events observed in the area C of Fig. 2, in which both $M_{K^+K^-}$ lie in the ϕ sideband region, we ignore this contribution.

The possible quantum electrodynamics (QED) processes under the $\psi(3686)$ peak consist of the peaking and nonpeaking parts. According to the Born cross sections measured by the BESIII [20] and Belle experiments [21] and the nominal solution below, the upper limits on the numbers of events at 90% confidence level are estimated to be less than 0.1 for the QED peaking $e^+e^- \to \gamma\chi_{cJ}$ processes, and thus their contributions can be negligible. The QED nonpeaking processes that do not have the χ_{cJ} signals, like $e^+e^- \to \gamma\phi\phi\eta$, can contribute to the flat distributions in Fig. 3. The QED processes are also studied using a 48.8 pb^{-1} off-resonance data sample taken at a center-of-mass energy of 3.65 GeV [22], where the scaling factor of the integrated luminosity is 0.07 compared with the $\psi(3686)$ data sample [8]. But no events survive after applying the same event selection criteria.

The signal yields are obtained from unbinned maximum likelihood fits to the $M_{\phi K^+K^-\gamma\gamma}$ spectra, where at least one of the ϕ candidates has an invariant mass within the signal window. The fits are performed in the R1, R2, and R3 regions, where the latter two regions correspond to the area A with $M_{\gamma\gamma}$ in the sideband regions, and the areas B with $M_{\gamma\gamma}$ in the signal region, respectively. In the fits, the signal shape in the $M_{\phi K^+K^-\gamma\gamma}$ distribution is extracted from signal MC simulations, and the background shape is modeled as a constant, where the background is from the events that do not form the χ_{cJ} signals, such as other $\psi(3686)$ decays and the possible QED nonpeaking processes. Figure 3 shows the fit results. The contribution of the areas B with $M_{\gamma\gamma}$ in the sideband region is negligible, since there are only two events. The signal yields for $\chi_{cJ} \to \phi\phi\eta$ decays are estimated by

$$N^{\rm sig}_{\rm obs} = N^{\rm R1}_{\rm obs} - f_{\rm R2} \cdot N^{\rm R2}_{\rm obs} - f_{\rm R3} \cdot N^{\rm R3}_{\rm obs}, \qquad (1)$$

where $N^r_{\rm obs}$ is the number of observed events for the corresponding r region ($r = R1$, R2, or R3), and both the normalization factors $f_{\rm R2}$ and $f_{\rm R3}$ are 1.0, which have

TABLE I. The numbers of observed events for different regions in $\chi_{cJ} \to \phi\phi\eta$ decays, as well as their statistical significances (Sig.). The errors are statistical only.

Mode	$N_{\rm obs}^{\rm R1}$	$N_{\rm obs}^{\rm R2}$	$N_{\rm obs}^{\rm R3}$	Sig.
χ_{c0}	201.2 ± 15.6	0.0 ± 0.9	14.6 ± 4.7	18σ
χ_{c1}	108.0 ± 11.0	8.6 ± 3.1	15.8 ± 4.2	10σ
χ_{c2}	160.7 ± 13.2	1.5 ± 1.5	15.6 ± 4.2	17σ

been evaluated from the ratios of the background yields in the η and 2D ϕ signal and sideband regions, respectively. The numbers of events obtained by the fits to $M_{\phi K^+K^-\gamma\gamma}$ in different regions for $\chi_{cJ} \to \phi\phi\eta$ decays are summarized in Table I, along with their statistical significances.

V. BRANCHING FRACTIONS

The branching fractions for $\chi_{cJ} \to \phi\phi\eta$ decays are determined by

$$\mathcal{B}_{\chi_{cJ}\to\phi\phi\eta} = \frac{N_{\rm obs}^{\rm sig}}{N_{\psi(3686)} \cdot \mathcal{B}_0 \cdot \epsilon}, \tag{2}$$

where $N_{\psi(3686)}$ is the total number of $\psi(3686)$ decays, $\mathcal{B}_0 = \mathcal{B}_{\psi(3686)\to\gamma\chi_{cJ}}\mathcal{B}^2_{\phi\to K^+K^-}\mathcal{B}_{\eta\to\gamma\gamma}$ is the product of the branching fractions cited from the world average values [1], and ϵ is the detection efficiency.

In order to obtain the best possible estimate for the detection efficiencies, the signal MC samples are corrected in two aspects:

(i) The track helix parameters [23] are modified to reduce the difference of the kinematic fit $\chi^2_{\rm 4C}$ between the data and MC sample, where the correction factors for their resolutions are obtained from a clean control sample of the $\psi(3686) \to K^+K^-\pi^+\pi^-$ decay.

(ii) Taking into account E1 transition effects on the line shapes of χ_{cJ} mesons generated with the Breit-Wigner functions, a weighting factor $(\frac{E_{\gamma 1}}{E_{\gamma 10}})^3$ [24] is applied to the $M_{\phi K^+K^-\gamma\gamma}$ spectra, where $E_{\gamma 1}$ is the radiative photon's energy in the rest frame of the $\psi(3686)$ meson without detector reconstruction effects, and $E_{\gamma 10}$ is the most probable transition energy,

$$E_{\gamma 10} = \frac{E^2_{\rm cms} - m^2_{\chi_{cJ}}}{2E_{\rm cms}}. \tag{3}$$

Here $m_{\chi_{cJ}}$ are the nominal masses of the χ_{cJ} mesons [1], and $E_{\rm cms}$ is the center-of-mass energy of 3.686 GeV. The detection efficiencies are determined to be $(5.30 \pm 0.02)\%$, $(6.77 \pm 0.03)\%$, and $(6.62 \pm 0.03)\%$ for χ_{c0}, χ_{c1}, and $\chi_{c2} \to \phi\phi\eta$ decays, respectively.

VI. SYSTEMATIC UNCERTAINTIES

The sources of systematic uncertainty include the total number of $\psi(3686)$ decays, the MDC tracking efficiency, PID efficiency, photon detection efficiency, η and ϕ mass requirements, kinematic fit, fit procedure, peaking background estimation, and cited branching fractions.

The total number of $\psi(3686)$ decays is $N_{\psi(3686)} = (448.1 \pm 2.9) \times 10^6$ [8], which is determined by counting hadronic events. The systematic uncertainty is 0.6%.

The control samples of $J/\psi \to K^0_S K^\pm \pi^\mp, K^0_S \to \pi^+\pi^-$ decays [25] have been used to investigate the MDC tracking efficiency, and the difference of 1% per $K^\pm$ track between the data and MC simulation is assigned as the systematic uncertainty. By means of the same control sample, the uncertainty due to PID efficiency is estimated to be also 1% per $K^\pm$ track. The systematic uncertainty from the photon detection efficiency is determined to be 1% per photon utilizing a control sample of $J/\psi \to \rho^0\pi^0$ with $\rho^0 \to \pi^+\pi^-$ and $\pi^0 \to \gamma\gamma$ [26].

The systematic uncertainty arising from the η (ϕ) mass requirement is evaluated by changing the mass resolution and shifting the mass window. In the nominal fit, the η signal shape is described as the shape derived from signal MC simulation convolved with a Gaussian function, and the ϕ signal shape is modeled as a P-wave Breit-Wigner function convolved with a Gaussian function. Alternative fits are performed by modeling the η signal shape with the shape from signal MC simulation, changing the width of the Gaussian function for the ϕ signal shape to that obtained from the signal MC sample, and varying the η (ϕ) mass window by the respective mass resolution obtained in the fit to the signal shape. The difference of the efficiency of the η (ϕ) mass requirement between the data and MC sample is taken as the systematic uncertainty from the η (ϕ) mass requirement.

In the nominal analysis, the track helix parameters for charged tracks from signal MC samples are modified to improve the agreement between the data and MC simulation. An alternative detection efficiency is obtained with no modification to the track helix parameters, and the difference is assigned as the systematic uncertainty associated with the kinematic fit.

The sources of systematic uncertainty from the fit procedure include the signal shape, background shape, and the fit range.

(i) In the nominal fit, the χ_{cJ} signal shape is modeled with the MC simulation. An alternative fit is performed with the MC simulation convolved with a Gaussian function with free width, and the difference of the signal yield is taken as the systematic uncertainty from the χ_{cJ} signal shape.

(ii) Different order Chebyshev functions instead of a constant are used in the alternative fits to describe the background. The largest difference of the signal

TABLE II. Relative systematic uncertainties on the measured branching fractions of $\chi_{cJ} \to \phi\phi\eta$ decays (in percent).

Source	χ_{c0}	χ_{c1}	χ_{c2}
$N_{\psi(3686)}$	0.6	0.6	0.6
MDC tracking	4.0	4.0	4.0
PID	4.0	4.0	4.0
Photon detection	3.0	3.0	3.0
η mass requirement	0.2	0.2	0.2
ϕ mass requirement	0.2	0.2	0.2
Kinematic fit	1.3	1.4	0.7
Fit procedure	1.0	0.9	1.2
Peaking backgrounds	1.3	0.9	0.9
Cited branching fractions	2.9	3.1	2.9
Total	7.4	7.4	7.3

yield is assigned as the systematic uncertainty from the background shape.

(iii) The fit ranges are varied from $[3.3, 3.6]$ GeV/c^2 to [3.25, 3.61] or $[3.35, 3.6]$ GeV/c^2. The largest difference of the signal yield is taken as the systematic uncertainty associated with the fit range.

The quadratic sum of the above three systematic uncertainties is taken as the systematic uncertainty from the fit procedure.

In the nominal fit, events in the η sideband and 2D ϕ sideband regions are used to estimate contributions from peaking background sources with no η signal and only one ϕ signal, respectively. Alternative fits are performed by varying the width of the η (ϕ) sideband regions within one standard deviation of the corresponding mass resolution, and the largest difference of the signal yield is taken as the corresponding systematic uncertainty. The quadratic sum of the two cases is taken as the systematic uncertainty from peaking backgrounds.

The uncertainties associated with the branching fractions of $\psi(3686) \to \gamma\chi_{cJ}$, $\phi \to K^+K^-$ and $\eta \to \gamma\gamma$ are extracted from the world average values [1]. The systematic uncertainty due to the trigger efficiency is negligible according to the studies in Ref. [27].

The total systematic uncertainty on the measured branching fractions for $\chi_{cJ} \to \phi\phi\eta$ decays is the quadratic sum of each individual contribution, as summarized in Table II.

VII. RESULTS AND DISCUSSION

The measured branching fractions of $\chi_{cJ} \to \phi\phi\eta$ decays are summarized in Table III, where the first uncertainties are statistical, and the second are systematic.

TABLE III. Summary of the resulting branching fractions for $\chi_{cJ} \to \phi\phi\eta$ decays.

Mode	$\mathcal{B}(\times 10^{-4})$
$\chi_{c0} \to \phi\phi\eta$	$8.41 \pm 0.74 \pm 0.62$
$\chi_{c1} \to \phi\phi\eta$	$2.96 \pm 0.43 \pm 0.22$
$\chi_{c2} \to \phi\phi\eta$	$5.33 \pm 0.52 \pm 0.39$

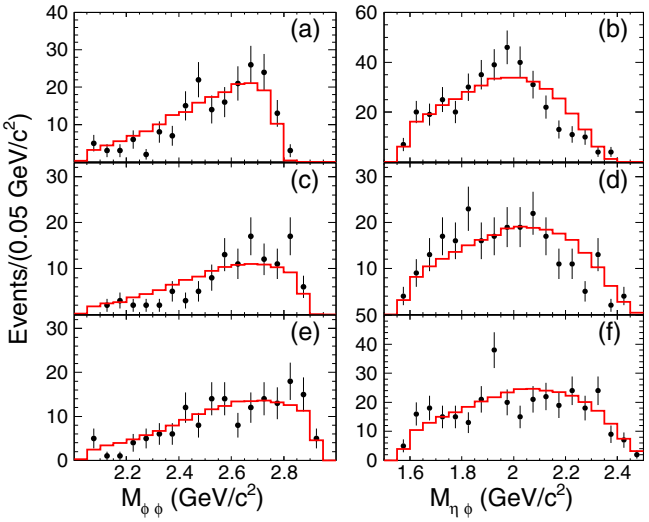

FIG. 5. Comparison of the $M_{\phi\phi}$ and $M_{\eta\phi}$ spectra for data (dots with error bars) and signal MC (solid red lines) samples within the (a),(b) χ_{c0}, (c),(d) χ_{c1}, and (e),(f) χ_{c2} signal regions.

Figure 5 shows the projections on the $M_{\phi\phi}$ and $M_{\eta\phi}$ spectra. There are two combinations of $M_{\eta\phi}$ for each event. Compared with those from the signal MC samples, some excesses in data are observed. However, considering the limited statistics, it is hard to draw a conclusion that intermediate states appear in $\chi_{cJ} \to \phi\phi\eta$ decays. Perhaps in the future, utilizing more data samples, it would be worthwhile to combine other ϕ and η decay modes, such as $\phi \to \pi^+\pi^-\pi^0$, $\phi \to K^0_S K^0_L$, and $\eta \to \pi^+\pi^-\pi^0$ decays, to perform a partial wave analysis of $\chi_{cJ} \to \phi\phi\eta$ decays, so that we can make clear conclusions on the existence of intermediate states.

VIII. SUMMARY

In summary, the decays $\chi_{cJ} \to \phi\phi\eta$ have been measured for the first time through $\psi(3686)$ radiative decays, based on 4.48×10^8 $\psi(3686)$ decays collected with the BESIII detector. The resulting branching fractions are $(8.41 \pm 0.74 \pm 0.62) \times 10^{-4}$, $(2.96 \pm 0.43 \pm 0.22) \times 10^{-4}$, and $(5.33 \pm 0.52 \pm 0.39) \times 10^{-4}$ for $\chi_{c0,1,2} \to \phi\phi\eta$ decays, where the first and second uncertainties are statistical and systematic, respectively. At the present level of statistics, no obvious resonant structure is observed in the $M_{\phi\phi}$ or $M_{\eta\phi}$ spectra.

ACKNOWLEDGMENTS

The BESIII Collaboration thanks the staff of BEPCII and the IHEP computing center for their strong support. This work is supported in part by National Key Basic Research Program of China under Contract No. 2015CB856700; National Natural Science Foundation of China (NSFC) under Contracts No. 11805037, No. 11625523, No. 11635010, No. 11735014, No. 11822506, and

No. 11835012; the Chinese Academy of Sciences (CAS) Large-Scale Scientific Facility Program; Joint Large-Scale Scientific Facility Funds of the NSFC and CAS under Contracts No. U1832121, No. U1632107, No. U1532257, No. U1532258, No. U1732263, and No. U1832207; CAS Key Research Program of Frontier Sciences under Contracts No. QYZDJ-SSW-SLH003 and No. QYZDJ-SSW-SLH040; 100 Talents Program of CAS; the Institute of Nuclear and Particle Physics (INPAC) and Shanghai Key Laboratory for Particle Physics and Cosmology; ERC under Contract No. 758462; German Research Foundation DFG under Contracts No. Collaborative Research Center CRC 1044 and No. FOR 2359; Istituto Nazionale di Fisica Nucleare, Italy; Koninklijke Nederlandse Akademie van Wetenschappen (KNAW) under Contract No. 530-4CDP03; Ministry of Development of Turkey under Contract No. DPT2006K-120470; National Science and Technology fund; STFC (United Kingdom); the Knut and Alice Wallenberg Foundation (Sweden) under Contract No. 2016.0157; the Royal Society, UK, under Contracts No. DH140054 and No. DH160214; the Swedish Research Council; U.S. Department of Energy under Contracts No. DE-FG02-05ER41374, No. DE-SC-0010118, and No. DE-SC-0012069; University of Groningen (RuG) and the Helmholtzzentrum fuer Schwerionenforschung GmbH (GSI), Darmstadt.

[1] M. Tanabashi *et al.* (Particle Data Group), Phys. Rev. D **98**, 030001 (2018).
[2] W. Braunschweig *et al.* (DASP Collaboration), Phys. Lett. **57B**, 407 (1975).
[3] G. J. Feldman *et al.* (Mark I Collaboration), Phys. Rev. Lett. **35**, 821 (1975).
[4] M. Ablikim *et al.* (BESIII Collaboration), Phys. Rev. D **93**, 112011 (2016).
[5] A. Etkin *et al.*, Phys. Rev. Lett. **41**, 784 (1978); Phys. Lett. **165B**, 217 (1985); Phys. Lett. B **201**, 568 (1988).
[6] C.-K. Chua, W.-S. Hou, and S.-Y. Tsai, Phys. Lett. B **544**, 139 (2002).
[7] H.-C. Huang *et al.* (Belle Collaboration), Phys. Rev. Lett. **91**, 241802 (2003); B. Aubert *et al.* (*BABAR* Collaboration), Phys. Rev. Lett. **97**, 261803 (2006); R. Aaij *et al.* (LHCb Collaboration), J. High Energy Phys. 03 (2016) 040.
[8] M. Ablikim *et al.* (BESIII Collaboration), Chin. Phys. C **42**, 023001 (2018).
[9] M. Ablikim *et al.* (BESIII Collaboration), Nucl. Instrum. Methods Phys. Res., Sect. A **614**, 345 (2010).
[10] C. H. Yu *et al.*, *Proceedings of IPAC2016, Busan, Korea* (2016), https://dx.doi.org/10.18429/JACoW-IPAC2016-TUYA01.
[11] S. Agostinelli *et al.* (GEANT4 Collaboration), Nucl. Instrum. Methods Phys. Res., Sect. A **506**, 250 (2003).
[12] S. Jadach, B. F. L. Ward, and Z. Was, Phys. Rev. D **63**, 113009 (2001); Comput. Phys. Commun. **130**, 260 (2000).
[13] D. J. Lange, Nucl. Instrum. Methods Phys. Res., Sect. A **462**, 152 (2001); R. G. Ping, Chin. Phys. C **32**, 599 (2008).
[14] J. C. Chen, G. S. Huang, X. R. Qi, D. H. Zhang, and Y. S. Zhu, Phys. Rev. D **62**, 034003 (2000); R. L. Yang, R. G. Ping, and H. Chen, Chin. Phys. Lett. **31**, 061301 (2014).
[15] E. Richter-Was, Phys. Lett. B **303**, 163 (1993).
[16] E. Eichten, S. Godfrey, H. Mahlke, and J. L. Rosner, Rev. Mod. Phys. **80**, 1161 (2008).
[17] M. Oreglia, E. Bloom, F. Bulos, R. Chestnut, J. Gaiser, G. Godfrey *et al.*, Phys. Rev. D **25**, 2259 (1982).
[18] G. Karl, S. Meshkov, and J. L. Rosner, Phys. Rev. D **13**, 1203 (1976).
[19] M. A. Doncheski, H. Grotch, and K. J. Sebastian, Phys. Rev. D **42**, 2293 (1990).
[20] M. Ablikim *et al.* (BESIII Collaboration), Chin. Phys. C **39**, 041001 (2015).
[21] Y. L. Han *et al.* (Belle Collaboration), Phys. Rev. D **92**, 012011 (2015).
[22] M. Ablikim *et al.* (BESIII Collaboration), Phys. Rev. D **96**, 112012 (2017).
[23] M. Ablikim *et al.* (BESIII Collaboration), Phys. Rev. D **87**, 012002 (2013).
[24] M. Ablikim *et al.* (BESIII Collaboration), Phys. Rev. D **96**, 092007 (2017).
[25] M. Ablikim *et al.* (BESIII Collaboration), Phys. Rev. D **87**, 052005 (2013).
[26] M. Ablikim *et al.* (BESIII Collaboration), Phys. Rev. D **81**, 052005 (2010).
[27] N. Berger, K. Zhu, Z.-A. Liu, D.-P. Jin, H. Xu, W.-X. Gong, K. Wang, and G.-F. Cao, Chin. Phys. C **34**, 1779 (2010).